BABAR-PUB-02/02
SLAC-PUB-9128

Measurement of the B^0 Lifetime with Partially Reconstructed $B^0 \to D^{*-}\ell^+\nu_\ell$ Decays

B. Aubert,[1] D. Boutigny,[1] J.-M. Gaillard,[1] A. Hicheur,[1] Y. Karyotakis,[1] J. P. Lees,[1] P. Robbe,[1] V. Tisserand,[1] A. Zghiche,[1] A. Palano,[2] A. Pompili,[2] G. P. Chen,[3] J. C. Chen,[3] N. D. Qi,[3] G. Rong,[3] P. Wang,[3] Y. S. Zhu,[3] G. Eigen,[4] B. Stugu,[4] G. S. Abrams,[5] A. W. Borgland,[5] A. B. Breon,[5] D. N. Brown,[5] J. Button-Shafer,[5] R. N. Cahn,[5] A. R. Clark,[5] M. S. Gill,[5] A. V. Gritsan,[5] Y. Groysman,[5] R. G. Jacobsen,[5] R. W. Kadel,[5] J. Kadyk,[5] L. T. Kerth,[5] Yu. G. Kolomensky,[5] J. F. Kral,[5] C. LeClerc,[5] M. E. Levi,[5] G. Lynch,[5] P. J. Oddone,[5] M. Pripstein,[5] N. A. Roe,[5] A. Romosan,[5] M. T. Ronan,[5] V. G. Shelkov,[5] A. V. Telnov,[5] W. A. Wenzel,[5] T. J. Harrison,[6] C. M. Hawkes,[6] D. J. Knowles,[6] S. W. O'Neale,[6] R. C. Penny,[6] A. T. Watson,[6] N. K. Watson,[6] T. Deppermann,[7] K. Goetzen,[7] H. Koch,[7] M. Kunze,[7] B. Lewandowski,[7] K. Peters,[7] H. Schmuecker,[7] M. Steinke,[7] N. R. Barlow,[8] W. Bhimji,[8] N. Chevalier,[8] P. J. Clark,[8] W. N. Cottingham,[8] B. Foster,[8] C. Mackay,[8] F. F. Wilson,[8] K. Abe,[9] C. Hearty,[9] T. S. Mattison,[9] J. A. McKenna,[9] D. Thiessen,[9] S. Jolly,[10] A. K. McKemey,[10] V. E. Blinov,[11] A. D. Bukin,[11] D. A. Bukin,[11] A. R. Buzykaev,[11] V. B. Golubev,[11] V. N. Ivanchenko,[11] A. A. Korol,[11] E. A. Kravchenko,[11] A. P. Onuchin,[11] S. I. Serednyakov,[11] Yu. I. Skovpen,[11] V. I. Telnov,[11] A. N. Yushkov,[11] D. Best,[12] M. Chao,[12] D. Kirkby,[12] A. J. Lankford,[12] M. Mandelkern,[12] S. McMahon,[12] D. P. Stoker,[12] K. Arisaka,[13] C. Buchanan,[13] S. Chun,[13] D. B. MacFarlane,[14] S. Prell,[14] Sh. Rahatlou,[14] G. Raven,[14] V. Sharma,[14] C. Campagnari,[15] B. Dahmes,[15] P. A. Hart,[15] N. Kuznetsova,[15] S. L. Levy,[15] O. Long,[15] A. Lu,[15] M. A. Mazur,[15] J. D. Richman,[15] W. Verkerke,[15] J. Beringer,[16] A. M. Eisner,[16] M. Grothe,[16] C. A. Heusch,[16] W. S. Lockman,[16] T. Pulliam,[16] T. Schalk,[16] R. E. Schmitz,[16] B. A. Schumm,[16] A. Seiden,[16] M. Turri,[16] W. Walkowiak,[16] D. C. Williams,[16] M. G. Wilson,[16] E. Chen,[17] G. P. Dubois-Felsmann,[17] A. Dvoretskii,[17] D. G. Hitlin,[17] S. Metzler,[17] J. Oyang,[17] F. C. Porter,[17] A. Ryd,[17] A. Samuel,[17] M. Weaver,[17] S. Yang,[17] R. Y. Zhu,[17] S. Devmal,[18] T. L. Geld,[18] S. Jayatilleke,[18] G. Mancinelli,[18] B. T. Meadows,[18] M. D. Sokoloff,[18] T. Barillari,[19] P. Bloom,[19] M. O. Dima,[19] W. T. Ford,[19] U. Nauenberg,[19] A. Olivas,[19] P. Rankin,[19] J. Roy,[19] J. G. Smith,[19] W. C. van Hoek,[19] J. Blouw,[20] J. L. Harton,[20] M. Krishnamurthy,[20] A. Soffer,[20] W. H. Toki,[20] R. J. Wilson,[20] J. Zhang,[20] T. Brandt,[21] J. Brose,[21] T. Colberg,[21] M. Dickopp,[21] R. S. Dubitzky,[21] A. Hauke,[21] E. Maly,[21] R. Müller-Pfefferkorn,[21] S. Otto,[21] K. R. Schubert,[21] R. Schwierz,[21] B. Spaan,[21] L. Wilden,[21] D. Bernard,[22] G. R. Bonneaud,[22] F. Brochard,[22] J. Cohen-Tanugi,[22] S. Ferrag,[22] S. T'Jampens,[22] Ch. Thiebaux,[22] G. Vasileiadis,[22] M. Verderi,[22] A. Anjomshoaa,[23] R. Bernet,[23] A. Khan,[23] D. Lavin,[23] F. Muheim,[23] S. Playfer,[23] J. E. Swain,[23] J. Tinslay,[23] M. Falbo,[24] C. Borean,[25] C. Bozzi,[25] S. Dittongo,[25] L. Piemontese,[25] E. Treadwell,[26] F. Anulli,[27,*] R. Baldini-Ferroli,[27] A. Calcaterra,[27] R. de Sangro,[27] D. Falciai,[27] G. Finocchiaro,[27] P. Patteri,[27] I. M. Peruzzi,[27,*] M. Piccolo,[27] Y. Xie,[27] A. Zallo,[27] S. Bagnasco,[28] A. Buzzo,[28] R. Contri,[28] G. Crosetti,[28] M. Lo Vetere,[28] M. Macri,[28] M. R. Monge,[28] S. Passaggio,[28] F. C. Pastore,[28] C. Patrignani,[28] M. G. Pia,[28] E. Robutti,[28] A. Santroni,[28] S. Tosi,[28] M. Morii,[29] R. Bartoldus,[30] R. Hamilton,[30] U. Mallik,[30] J. Cochran,[31] H. B. Crawley,[31] P.-A. Fischer,[31] J. Lamsa,[31] W. T. Meyer,[31] E. I. Rosenberg,[31] G. Grosdidier,[32] C. Hast,[32] A. Höcker,[32] H. M. Lacker,[32] S. Laplace,[32] V. Lepeltier,[32] A. M. Lutz,[32] S. Plaszczynski,[32] M. H. Schune,[32] S. Trincaz-Duvoid,[32] G. Wormser,[32] R. M. Bionta,[33] V. Brigljević,[33] D. J. Lange,[33] M. Mugge,[33] K. van Bibber,[33] D. M. Wright,[33] A. J. Bevan,[34] J. R. Fry,[34] E. Gabathuler,[34] R. Gamet,[34] M. George,[34] M. Kay,[34] D. J. Payne,[34] R. J. Sloane,[34] C. Touramanis,[34] M. L. Aspinwall,[35] D. A. Bowerman,[35] P. D. Dauncey,[35] U. Egede,[35] I. Eschrich,[35] N. J. W. Gunawardane,[35] J. A. Nash,[35] P. Sanders,[35] D. Smith,[35] D. E. Azzopardi,[36] J. J. Back,[36] G. Bellodi,[36] P. Dixon,[36] P. F. Harrison,[36] R. J. L. Potter,[36] H. W. Shorthouse,[36] P. Strother,[36] P. B. Vidal,[36] G. Cowan,[37] S. George,[37] M. G. Green,[37] A. Kurup,[37] C. E. Marker,[37] P. McGrath,[37] T. R. McMahon,[37] S. Ricciardi,[37] F. Salvatore,[37] G. Vaitsas,[37] D. Brown,[38] C. L. Davis,[38] J. Allison,[39] R. J. Barlow,[39] J. T. Boyd,[39] A. C. Forti,[39] J. Fullwood,[39] F. Jackson,[39] G. D. Lafferty,[39] N. Savvas,[39] J. H. Weatherall,[39] J. C. Williams,[39] A. Farbin,[40] A. Jawahery,[40] V. Lillard,[40] J. Olsen,[40] D. A. Roberts,[40] J. R. Schieck,[40] G. Blaylock,[41] C. Dallapiccola,[41] K. T. Flood,[41] S. S. Hertzbach,[41] R. Kofler,[41] V. G. Koptchev,[41] T. B. Moore,[41] H. Staengle,[41] S. Willocq,[41] B. Brau,[42] R. Cowan,[42] G. Sciolla,[42] F. Taylor,[42] R. K. Yamamoto,[42] M. Milek,[43] P. M. Patel,[43] F. Palombo,[44] J. M. Bauer,[45] L. Cremaldi,[45] V. Eschenburg,[45] R. Kroeger,[45] J. Reidy,[45] D. A. Sanders,[45] D. J. Summers,[45] J. Y. Nief,[46] P. Taras,[46] H. Nicholson,[47] C. Cartaro,[48] N. Cavallo,[48,†] G. De Nardo,[48] F. Fabozzi,[48] C. Gatto,[48]

L. Lista,[48] P. Paolucci,[48] D. Piccolo,[48] C. Sciacca,[48] J. M. LoSecco,[49] J. R. G. Alsmiller,[50] T. A. Gabriel,[50] J. Brau,[51] R. Frey,[51] E. Grauges,[51] M. Iwasaki,[51] N. B. Sinev,[51] D. Strom,[51] F. Colecchia,[52] F. Dal Corso,[52] A. Dorigo,[52] F. Galeazzi,[52] M. Margoni,[52] G. Michelon,[52] M. Morandin,[52] M. Posocco,[52] M. Rotondo,[52] F. Simonetto,[52] R. Stroili,[52] E. Torassa,[52] C. Voci,[52] M. Benayoun,[53] H. Briand,[53] J. Chauveau,[53] P. David,[53] Ch. de la Vaissière,[53] L. Del Buono,[53] O. Hamon,[53] F. Le Diberder,[53] Ph. Leruste,[53] J. Ocariz,[53] L. Roos,[53] J. Stark,[53] P. F. Manfredi,[54] V. Re,[54] V. Speziali,[54] E. D. Frank,[55] L. Gladney,[55] Q. H. Guo,[55] J. Panetta,[55] C. Angelini,[56] G. Batignani,[56] S. Bettarini,[56] M. Bondioli,[56] F. Bucci,[56] E. Campagna,[56] M. Carpinelli,[56] F. Forti,[56] M. A. Giorgi,[56] A. Lusiani,[56] G. Marchiori,[56] F. Martinez-Vidal,[56] M. Morganti,[56] N. Neri,[56] E. Paoloni,[56] M. Rama,[56] G. Rizzo,[56] F. Sandrelli,[56] G. Simi,[56] G. Triggiani,[56] J. Walsh,[56] M. Haire,[57] D. Judd,[57] K. Paick,[57] L. Turnbull,[57] D. E. Wagoner,[57] J. Albert,[58] P. Elmer,[58] C. Lu,[58] V. Miftakov,[58] S. F. Schaffner,[58] A. J. S. Smith,[58] A. Tumanov,[58] E. W. Varnes,[58] G. Cavoto,[59] D. del Re,[59] R. Faccini,[14,59] F. Ferrarotto,[59] F. Ferroni,[59] E. Lamanna,[59] M. A. Mazzoni,[59] S. Morganti,[59] G. Piredda,[59] F. Safai Tehrani,[59] M. Serra,[59] C. Voena,[59] S. Christ,[60] R. Waldi,[60] T. Adye,[61] N. De Groot,[61] B. Franek,[61] N. I. Geddes,[61] G. P. Gopal,[61] S. M. Xella,[61] R. Aleksan,[62] S. Emery,[62] A. Gaidot,[62] S. F. Ganzhur,[62] P.-F. Giraud,[62] G. Hamel de Monchenault,[62] W. Kozanecki,[62] M. Langer,[62] G. W. London,[62] B. Mayer,[62] B. Serfass,[62] G. Vasseur,[62] Ch. Yèche,[62] M. Zito,[62] M. V. Purohit,[63] H. Singh,[63] A. W. Weidemann,[63] F. X. Yumiceva,[63] I. Adam,[64] D. Aston,[64] N. Berger,[64] A. M. Boyarski,[64] G. Calderini,[64] M. R. Convery,[64] D. P. Coupal,[64] D. Dong,[64] J. Dorfan,[64] W. Dunwoodie,[64] R. C. Field,[64] T. Glanzman,[64] S. J. Gowdy,[64] T. Haas,[64] V. Halyo,[64] T. Himel,[64] T. Hryn'ova,[64] M. E. Huffer,[64] W. R. Innes,[64] C. P. Jessop,[64] M. H. Kelsey,[64] P. Kim,[64] M. L. Kocian,[64] U. Langenegger,[64] D. W. G. S. Leith,[64] S. Luitz,[64] V. Luth,[64] H. L. Lynch,[64] H. Marsiske,[64] S. Menke,[64] R. Messner,[64] D. R. Muller,[64] C. P. O'Grady,[64] V. E. Ozcan,[64] A. Perazzo,[64] M. Perl,[64] S. Petrak,[64] H. Quinn,[64] B. N. Ratcliff,[64] S. H. Robertson,[64] A. Roodman,[64] A. A. Salnikov,[64] T. Schietinger,[64] R. H. Schindler,[64] J. Schwiening,[64] A. Snyder,[64] A. Soha,[64] S. M. Spanier,[64] J. Stelzer,[64] D. Su,[64] M. K. Sullivan,[64] H. A. Tanaka,[64] J. Va'vra,[64] S. R. Wagner,[64] A. J. R. Weinstein,[64] W. J. Wisniewski,[64] D. H. Wright,[64] C. C. Young,[64] P. R. Burchat,[65] C. H. Cheng,[65] T. I. Meyer,[65] C. Roat,[65] R. Henderson,[66] W. Bugg,[67] H. Cohn,[67] J. M. Izen,[68] I. Kitayama,[68] X. C. Lou,[68] F. Bianchi,[69] M. Bona,[69] D. Gamba,[69] L. Bosisio,[70] G. Della Ricca,[70] L. Lanceri,[70] P. Poropat,[70] G. Vuagnin,[70] R. S. Panvini,[71] C. M. Brown,[72] P. D. Jackson,[72] R. Kowalewski,[72] J. M. Roney,[72] H. R. Band,[73] E. Charles,[73] S. Dasu,[73] A. M. Eichenbaum,[73] H. Hu,[73] J. R. Johnson,[73] R. Liu,[73] F. Di Lodovico,[73] Y. Pan,[73] R. Prepost,[73] I. J. Scott,[73] S. J. Sekula,[73] J. H. von Wimmersperg-Toeller,[73] S. L. Wu,[73] Z. Yu,[73] T. M. B. Kordich,[74] and H. Neal[74]

(The *BABAR* Collaboration)

[1] *Laboratoire de Physique des Particules, F-74941 Annecy-le-Vieux, France*
[2] *Università di Bari, Dipartimento di Fisica and INFN, I-70126 Bari, Italy*
[3] *Institute of High Energy Physics, Beijing 100039, China*
[4] *University of Bergen, Inst. of Physics, N-5007 Bergen, Norway*
[5] *Lawrence Berkeley National Laboratory and University of California, Berkeley, CA 94720, USA*
[6] *University of Birmingham, Birmingham, B15 2TT, United Kingdom*
[7] *Ruhr Universität Bochum, Institut für Experimentalphysik 1, D-44780 Bochum, Germany*
[8] *University of Bristol, Bristol BS8 1TL, United Kingdom*
[9] *University of British Columbia, Vancouver, BC, Canada V6T 1Z1*
[10] *Brunel University, Uxbridge, Middlesex UB8 3PH, United Kingdom*
[11] *Budker Institute of Nuclear Physics, Novosibirsk 630090, Russia*
[12] *University of California at Irvine, Irvine, CA 92697, USA*
[13] *University of California at Los Angeles, Los Angeles, CA 90024, USA*
[14] *University of California at San Diego, La Jolla, CA 92093, USA*
[15] *University of California at Santa Barbara, Santa Barbara, CA 93106, USA*
[16] *University of California at Santa Cruz, Institute for Particle Physics, Santa Cruz, CA 95064, USA*
[17] *California Institute of Technology, Pasadena, CA 91125, USA*
[18] *University of Cincinnati, Cincinnati, OH 45221, USA*
[19] *University of Colorado, Boulder, CO 80309, USA*
[20] *Colorado State University, Fort Collins, CO 80523, USA*
[21] *Technische Universität Dresden, Institut für Kern- und Teilchenphysik, D-01062, Dresden, Germany*
[22] *Ecole Polytechnique, F-91128 Palaiseau, France*
[23] *University of Edinburgh, Edinburgh EH9 3JZ, United Kingdom*
[24] *Elon University, Elon University, NC 27244-2010, USA*
[25] *Università di Ferrara, Dipartimento di Fisica and INFN, I-44100 Ferrara, Italy*
[26] *Florida A&M University, Tallahassee, FL 32307, USA*

[27]Laboratori Nazionali di Frascati dell'INFN, I-00044 Frascati, Italy
[28]Università di Genova, Dipartimento di Fisica and INFN, I-16146 Genova, Italy
[29]Harvard University, Cambridge, MA 02138, USA
[30]University of Iowa, Iowa City, IA 52242, USA
[31]Iowa State University, Ames, IA 50011-3160, USA
[32]Laboratoire de l'Accélérateur Linéaire, F-91898 Orsay, France
[33]Lawrence Livermore National Laboratory, Livermore, CA 94550, USA
[34]University of Liverpool, Liverpool L69 3BX, United Kingdom
[35]University of London, Imperial College, London, SW7 2BW, United Kingdom
[36]Queen Mary, University of London, E1 4NS, United Kingdom
[37]University of London, Royal Holloway and Bedford New College, Egham, Surrey TW20 0EX, United Kingdom
[38]University of Louisville, Louisville, KY 40292, USA
[39]University of Manchester, Manchester M13 9PL, United Kingdom
[40]University of Maryland, College Park, MD 20742, USA
[41]University of Massachusetts, Amherst, MA 01003, USA
[42]Massachusetts Institute of Technology, Laboratory for Nuclear Science, Cambridge, MA 02139, USA
[43]McGill University, Montréal, QC, Canada H3A 2T8
[44]Università di Milano, Dipartimento di Fisica and INFN, I-20133 Milano, Italy
[45]University of Mississippi, University, MS 38677, USA
[46]Université de Montréal, Laboratoire René J. A. Lévesque, Montréal, QC, Canada H3C 3J7
[47]Mount Holyoke College, South Hadley, MA 01075, USA
[48]Università di Napoli Federico II, Dipartimento di Scienze Fisiche and INFN, I-80126, Napoli, Italy
[49]University of Notre Dame, Notre Dame, IN 46556, USA
[50]Oak Ridge National Laboratory, Oak Ridge, TN 37831, USA
[51]University of Oregon, Eugene, OR 97403, USA
[52]Università di Padova, Dipartimento di Fisica and INFN, I-35131 Padova, Italy
[53]Universités Paris VI et VII, Lab de Physique Nucléaire H. E., F-75252 Paris, France
[54]Università di Pavia, Dipartimento di Elettronica and INFN, I-27100 Pavia, Italy
[55]University of Pennsylvania, Philadelphia, PA 19104, USA
[56]Università di Pisa, Scuola Normale Superiore and INFN, I-56010 Pisa, Italy
[57]Prairie View A&M University, Prairie View, TX 77446, USA
[58]Princeton University, Princeton, NJ 08544, USA
[59]Università di Roma La Sapienza, Dipartimento di Fisica and INFN, I-00185 Roma, Italy
[60]Universität Rostock, D-18051 Rostock, Germany
[61]Rutherford Appleton Laboratory, Chilton, Didcot, Oxon, OX11 0QX, United Kingdom
[62]DAPNIA, Commissariat à l'Energie Atomique/Saclay, F-91191 Gif-sur-Yvette, France
[63]University of South Carolina, Columbia, SC 29208, USA
[64]Stanford Linear Accelerator Center, Stanford, CA 94309, USA
[65]Stanford University, Stanford, CA 94305-4060, USA
[66]TRIUMF, Vancouver, BC, Canada V6T 2A3
[67]University of Tennessee, Knoxville, TN 37996, USA
[68]University of Texas at Dallas, Richardson, TX 75083, USA
[69]Università di Torino, Dipartimento di Fisica Sperimentale and INFN, I-10125 Torino, Italy
[70]Università di Trieste, Dipartimento di Fisica and INFN, I-34127 Trieste, Italy
[71]Vanderbilt University, Nashville, TN 37235, USA
[72]University of Victoria, Victoria, BC, Canada V8W 3P6
[73]University of Wisconsin, Madison, WI 53706, USA
[74]Yale University, New Haven, CT 06511, USA

(Dated: February 7, 2008)

The B^0 lifetime has been measured with a sample of 23 million $B\overline{B}$ pairs collected by the *BABAR* detector at the PEP-II e^+e^- storage ring during 1999 and 2000. Events from the semileptonic decay $B^0 \to D^{*-}\ell^+\nu_\ell$ have been selected with a partial reconstruction method in which only the charged lepton and the slow π from the $D^{*-} \to \overline{D}^0\pi^-$ decay are reconstructed. The result is

$$\tau_{B^0} = 1.529 \pm 0.012 \text{ (stat)} \pm 0.029 \text{ (syst) ps.}$$

PACS numbers: 13.25.Hw, 12.15.Hh, 11.30.Er

The technique of partial reconstruction of D^{*-} mesons (charge conjugate states are always implied), in which only the slow pion from the $D^{*-} \to \overline{D}^0\pi^-$ decay is required, has been widely used in the past [1] to select large samples of reconstructed B mesons. This technique provides a way to measure the combination of CKM angles $(2\beta + \gamma)$ with $B^0 \to D^{*-}\pi^+$ decays [2]. The application of this method to the semileptonic decay $B^0 \to D^{*-}\ell^+\nu_\ell$

allows the method's validation, while providing a tool for precise measurements of several properties of the B^0, including its lifetime, τ_{B^0} , and the $B^0\overline{B}^0$ mixing parameter, Δm_d. A precise measurement of τ_{B^0} is presented herein.

The data used in this analysis, recorded by the *BABAR* detector at the PEP-II storage ring during 1999-2000, correspond to an integrated luminosity of 20.7 fb^{-1} collected on the $\Upsilon(4S)$ resonance (on-peak events) and 2.6 fb^{-1} collected 40 MeV below the resonance (off-peak) for background studies. Samples of simulated $B\overline{B}$ events were analyzed through the same analysis chain as the real data. The equivalent luminosity of the simulated data is approximately equal to the on-peak data.

A detailed description of the *BABAR* detector and the algorithms used for track reconstruction, particle identification, and selection of $B\overline{B}$ events is provided elsewhere [3]; a brief summary is given here. Particles with momenta $p \gtrsim 170\,\mathrm{MeV}/c$ are reconstructed by matching hits in the silicon vertex tracker (SVT) with track elements in the drift chamber (DCH). Since lower momentum tracks do not leave signals on many wires in the DCH due to the bending induced by the magnetic field, they are reconstructed by the SVT alone. Electrons are identified with the ratio of the track momentum to the associated energy deposited in the calorimeter (EMC), the transverse profile of the shower, the energy loss in the drift chamber, and the information from the Cherenkov detector (DIRC). The efficiency for electron identification in the acceptance of the electromagnetic calorimeter is about 90%, with a hadron misidentification probability equal to 0.15%. Muon candidates are required to have a path length and hit distribution in the instrumented flux return and energy deposition in the EMC consistent with that expected for a minimum-ionizing particle. The Cherenkov light emission in the DIRC is then employed to further reject kaons misidentified as muons, by requiring muon candidates to have a kaon hypothesis probability less than 5%. These criteria yield 74% muon efficiency with 2.6% hadron misidentification probability.

Semileptonic B^0 decays are then selected by searching for the high momentum charged lepton ($\ell = e, \mu$) from the B^0 decay and the slow pion (π_s) from the $D^{*-} \to \overline{D}^0\pi_s^-$ decay. To reject leptons from semileptonic charm decay and misidentified hadrons, the momentum of the lepton candidate in the $\Upsilon(4S)$ rest frame (p^*_ℓ) is required to be in the range $1.4 < p^*_\ell < 2.3$ GeV/c; that of the π_s ($p^*_{\pi_s}$) has to be less than 0.19 GeV/c. The kinematics of the decay are exploited for further background suppression as follows. As a consequence of the limited phase space available in the decay $D^{*-} \to \overline{D}^0\pi_s^-$, the π_s is emitted within a one-radian wide cone centered about the D^{*-} direction in the $\Upsilon(4S)$ rest frame. The D^{*-} four-momentum can therefore be computed by approximating its direction as that of the π_s, and parameterizing its momentum as a linear function of the π_s momentum, with parameters obtained from the simulation. The neutrino invariant mass can be computed from the four-momenta of the B^0, D^{*-}, and ℓ with the relation

$$M_\nu{}^2 = (P_{B^0} - P_{D^{*-}} - P_\ell)^2.$$

The momentum of the B^0 in the $\Upsilon(4S)$ rest frame, on average 0.34 GeV/c, is neglected. $M_\nu{}^2$ peaks approximately at zero for signal events, whereas background events are spread over a wide range.

TABLE I: Composition of the data sample in the signal region. The error is the sum in quadrature of the statistical and systematic errors from the fit to the data $M_\nu{}^2$ distribution.

Sample	# of events	Fraction (%)
Signal Region	172,700	-
Backgrounds		
Continuum	$19,600 \pm 400$	11.4 ± 0.2
$B\overline{B}$ comb.	$52,700 \pm 1,400$	30.0 ± 0.8
B^+	$8,700 \pm 4,400$	5.0 ± 2.5
B^0 signal	$91,700 \pm 4,600$	53.6 ± 2.6

The B^0 decay point is determined from a vertex fit of the π_s and ℓ tracks, constrained to the beam spot position in the plane perpendicular to the beam axis (the x-y plane). The beam spot is determined on a run-by-run basis using two-prong events [3]. Its size in the horizontal direction is 120 μm. Although the beam spot size in the vertical (y) direction is only 5.6 μm, a beam spot constraint of 50 μm is applied to account for the flight of the B^0 in the x-y plane. Only events for which the χ^2 probability of the vertex fit, $\mathcal{P}_V$, is greater than 0.1% are retained.

A selection is applied on the combined likelihood for p^*_ℓ, $p^*_{\pi_s}$, and $\mathcal{P}_V$, which results in a signal-to-background ratio of about one to one in the signal $M_\nu{}^2$ region, defined as $M_\nu{}^2 > -2$ GeV$^2/c^4$. Figure 1 shows the $M_\nu{}^2$ distribution of data events used to measure τ_{B^0} when the ℓ and the π_s have opposite-sign charges. Same-sign events are used as a background control sample. The individual distributions shown in Fig. 1 are obtained by fitting to the data the contributions from continuum events, obtained from the off-peak data, and from $B\overline{B}$ combinatorial background, B^0 signal, and B^+ resonant background, as predicted by the simulation. The B^+ resonant background is due to intermediate production of higher mass charm resonances (denoted as D^{**}). The fit determines the composition of the selected sample, which is reported in Table I for the events in the signal region.

The PEP-II collider produces $B\overline{B}$ pairs moving along the beam axis (z direction) with an average Lorentz boost of $\langle\beta\gamma\rangle = 0.55$. Hence, the two B decay vertices are separated on average by $\langle\Delta z\rangle \approx 255$ μm. The position of the $B^0 \to D^{*-}\ell^+\nu_\ell$ ("decay") vertex is reconstructed as described above. The decay point of the other B is determined from a selection of the remaining tracks in the

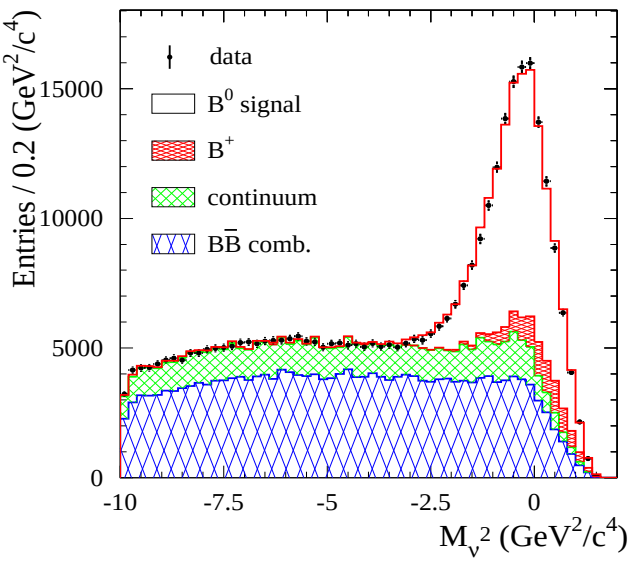

FIG. 1: The $M_\nu{}^2$ spectrum of the selected events. The data are represented by the dots with error bars. The result of the fit with shapes from the simulation are overlaid.

event using the following criteria. In events that have another lepton with momentum $p^* > 1.1\,\text{GeV}/c$, the other B vertex is computed with only this lepton track constrained to the beam-spot in the x-y plane. Otherwise, all the tracks with a center-of-mass angle greater than 90° with respect to the π_s direction are considered. This requirement is used to remove most of the tracks from the decay of the $\overline{D}{}^0$ daughter of the D^{*-}, which would otherwise bias the reconstruction of the other B vertex position. Simulation shows that in about 75% of signal events the other vertex has no tracks from the $\overline{D}{}^0$ decay. The selected tracks are then constrained to the beam-spot in the x-y plane. The track with the largest contribution to the vertex χ^2, if greater than 6, is removed and the fit iterated until no track fails this requirement. Vertices composed of just one track that is not a high momentum lepton are rejected in order to reduce the number of poorly measured vertices. The lifetime is determined by measuring the quantity $\Delta z = z_{\text{decay}} - z_{\text{other}}$, where $z_{\text{decay}}(z_{\text{other}})$ is the position along the beam line of the decay (other) vertex. The proper time difference is then computed with the relation $\Delta t = \Delta z/(c\beta\gamma)$. A fit with a double Gaussian to the Δt residuals in the Monte Carlo simulation shows that one half of the events are contained in the narrower Gaussian, which has a width of 0.7 ps. To remove badly reconstructed vertices, all events for which either $|\Delta z| > 3$ mm or $\sigma_{\Delta z} > 500$ μm are rejected, where $\sigma_{\Delta z}$ is the uncertainty on Δz computed for each event.

τ_{B^0} is obtained from a binned maximum likelihood fit to the two-dimensional $\Delta t, \sigma_{\Delta t}$ distribution. To save computation time events are grouped in a two-dimensional space consisting of 100 Δt and 25 $\sigma_{\Delta t}$ bins. The Δt distribution of signal events, $\mathcal{F}(\Delta t, \sigma_{\Delta t}, \tau_{B^0})$, is described by the convolution of the decay probability distribution

$$f(\Delta t_{\text{true}}|\tau_{B^0}) = \frac{1}{2\tau_{B^0}} exp(-|\Delta t_{\text{true}}|/\tau_{B^0}),$$

with the experimental resolution function, which is parametrized by the sum of three Gaussian distributions. The two narrow Gaussians, which account for more than 99% of the events, have the form

$$\mathcal{G}(\delta(\Delta t), \sigma_{\Delta t}) \equiv \frac{1}{\sqrt{2\pi} S \sigma_{\Delta t}} exp(-\frac{(\delta(\Delta t) - b)^2}{2S^2\sigma_{\Delta t}^2}) \ ,$$

where $\delta(\Delta t) = \Delta t - \Delta t_{\text{true}}$ is the difference between the measured and the true value of Δt, b is a bias due to the charm tracks in the other vertex and resolution effects, and the scale factor S is introduced to account for possible misestimation of the calculated error $\sigma_{\Delta t}$ on the proper time difference. The third Gaussian of fixed bias (-2 ps) and width (8 ps) is added to account for badly measured events ("outliers").

B^+ background events that peak in the $M_\nu{}^2$ signal region are described by an identical function, with the same resolution parameters as for the B^0 signal events, and an effective B^+ lifetime of 1.57 ps. This value, obtained by fitting simulated B^+ events, is smaller than the value of 1.655 ps generated in the simulation due to $\overline{D}{}^0$ tracks from the decay vertex being included in the other vertex.

The Δt distribution of continuum background events is modeled as the sum of two components, one with non-zero lifetime and the other with zero lifetime, convolved with the same single Gaussian resolution function. The parameters of the resolution function, as well as the lifetime and the fraction of events with non-zero lifetime, are all determined with the off-peak events that satisfy the selection criteria.

The Δt distribution of the combinatorial $B\overline{B}$ background is modeled as the sum of a non-zero and a zero-lifetime component, with a resolution function that is the sum of three Gaussians. All parameters are determined from the data by fitting the measured Δt distribution of the events in the sideband region, defined by $-10 < M_\nu{}^2 < -4\ \text{GeV}^2/c^4$. The Monte Carlo simulation shows, however, that there are small differences in the lifetime and in the fraction of events with non-zero lifetime between the signal region and the sideband. These differences are also observed in the data by separately fitting signal region and sideband events in the same sign $\ell\pi_s$ background control sample. The results from the like-sign fits are used to scale the two background parameters from the sideband to the signal region.

The function used to fit the data is the weighted sum of the four contributions:

$$\mathcal{F}(\Delta t, \sigma_{\Delta t}|\tau_{B^0}) = [1 - f_{B^+}({M_\nu}^2) - f_c({M_\nu}^2) - f_{B\overline{B}}({M_\nu}^2)]\,\mathcal{F}_{B^0}(\Delta t, \sigma_{\Delta t}, \tau_{B^0}) + f_{B^+}({M_\nu}^2)\,\mathcal{F}_{B^+}(\Delta t, \sigma_{\Delta t}) + f_c({M_\nu}^2)\,\mathcal{F}_c\,(\Delta t, \sigma_{\Delta t}) + f_{B\overline{B}}({M_\nu}^2)\,\mathcal{F}_{B\overline{B}}(\Delta t, \sigma_{\Delta t}),$$

where the functions $\mathcal{F}_{B^0}$, $\mathcal{F}_{B^+}$, $\mathcal{F}_c$ and $\mathcal{F}_{B\overline{B}}$ describe the measured decay time difference distributions for the signal, peaking B^+, continuum, and $B\overline{B}$ combinatorial background, respectively. f_{B^+}, f_c and $f_{B\overline{B}}$ are the probabilities that the event is from the B^+, continuum, or $B\overline{B}$ background, computed for each event on the basis of the measured value of ${M_\nu}^2$. Simultaneously with τ_{B^0}, the following parameters of the signal resolution function are fitted: the scale factor of the first Gaussian, $S_1 = 1.02 \pm 0.02$, the scale factor of the second Gaussian, $S_2 = 2.4 \pm 0.1$, the bias of the first Gaussian, $b_1 = -0.120 \pm 0.009$, and the fraction of outliers, $f_o = (0.2 \pm 0.1)\%$. The fraction of events contained in the second Gaussian, f_2, and its bias b_2 are fixed to 7% and -0.85 ps, respectively.

The result of the fit is $\tau_{B^0}^{\rm raw} = 1.482 \pm 0.012$ ps, where the error is statistical only. Figure 2 shows the comparison between the measured Δt distribution and the fit result. The probability of obtaining a lower likelihood, evaluated with a Monte Carlo technique, is 18%. This raw lifetime must be corrected for the bias induced by the tracks from the $\overline{D}^0$ that are not rejected by the π_s cone cut. A multiplicative correction factor of $\mathcal{R}_{\overline{D}^0} = 1.032 \pm 0.007({\rm stat}) \pm 0.007({\rm syst})$ is computed from the simulation. The statistical error arises from the number of simulated events. The dominant systematic uncertainty corresponds to the full variation in $\mathcal{R}_{\overline{D}^0}$ (0.66%) obtained by smearing the Δt resolution in the simulation to match that in the data. A second systematic uncertainty is computed by comparing in data and simulation the fraction of charged tracks from $\overline{D}^0$ decays outside the π_s cone for a subset of events in which the $\overline{D}^0$ is fully reconstructed in the $K^+\pi^-$, $K^+\pi^-\pi^0$, and $K^+\pi^-\pi^+\pi^-$ final states. The maximum discrepancy between data and simulation corresponds to a variation of $\pm 0.24\%$ in the value of $\mathcal{R}_{\overline{D}^0}$. The corrected value of the B^0 lifetime is then

$$\tau_{B^0} = \tau_{B^0}^{\rm raw}\mathcal{R}_{\overline{D}^0} = 1.529 \pm 0.012\,{\rm ps}.$$

The systematic error on τ_{B^0} is computed by adding in quadrature the contributions from several sources, described below and summarized in Table II.

The fractions of B^+, continuum, and combinatorial $B\overline{B}$ events are varied by the uncertainties obtained from the ${M_\nu}^2$ fit (see Table I). The parameters of the continuum and combinatorial $B\overline{B}$ Δt distributions are varied by their uncertainties, accounting for their correlations. As described above, the fraction of events with non-zero lifetime and the lifetime of the combinatorial $B\overline{B}$ background computed from the sideband are corrected with the same-sign control sample. This method is validated by a simulation study, and the statistical error of the validation is included in the background systematic error. The effective B^+ lifetime is varied by $\pm 3\%$, which is the sum in quadrature of the world average error on the B^+ lifetime and the statistical and systematic uncertainties of the $\overline{D}^0$ bias correction.

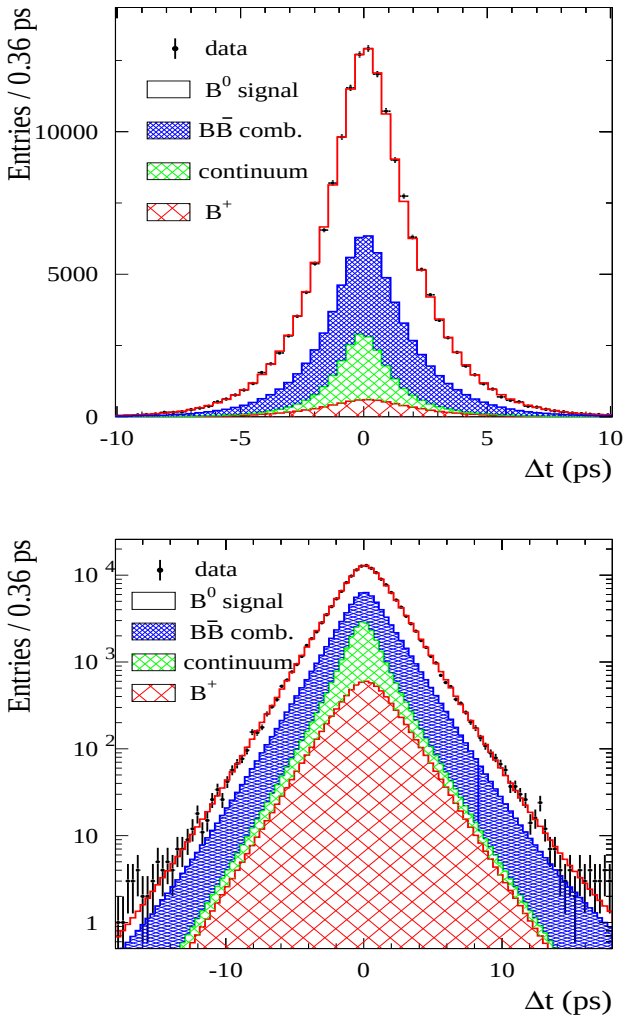

FIG. 2: Δt distribution for selected events in the data (points) in linear (upper) and logarithmic (lower) scale. The lifetime fit result is superimposed on the data. The hatched histograms show the contributions from the background sources described in the text.

The parameters of the signal resolution function that are not determined in the fit to the data are varied within conservative ranges (f_2 between 0.03 and 0.13, and b_2 between -1.5 and 0 ps). Several different analytical expressions are used to represent the small fraction of outliers. The fit is also performed by allowing the scale factor and the bias of the narrow Gaussians to depend linearly on $\sigma_{\Delta t}$ or on the lepton polar angle. The maximum change with respect to the result with fixed parameters is taken as the systematic error due to the parametrization of the resolution function.

The bias due to the event selection is found to be compatible with zero by fitting with an exponential function the true proper time difference of signal events selected in the simulation. The statistical error of this test is added to the systematic error.

The statistical and systematic errors on $\mathcal{R}_{\overline{D}^0}$ are propagated to the final error. A possible bias induced by the presence of tracks from charm decays produced by the other B meson is investigated in the simulation by varying within their uncertainties the relative fractions of charmless, single charm, and double charm events, and also by varying the relative fractions of D^+, D^0, D_s, and Λ_c hadrons. The z length scale is determined with an uncertainty of 0.4% from secondary interactions with a beam pipe section of known length. The dependence of the result on several different variables (angular width of the π_s cone used to reject $\overline{D}^0$ tracks, soft pion momentum, lepton momentum, polar and azimuthal angle, alignment conditions) is carefully inspected; no statistically significant effect is found. No difference in the result is observed if τ_{B^0} is determined with an unbinned maximum likelihood fit. A final relative error of $\pm 1.9\%$ is found by adding in quadrature the uncertainties from the above sources, as listed in Table II.

In conclusion, a sample of about 92000 $B^0 \to D^{*-}\ell^+\nu_\ell$ decays is selected by partial reconstruction of the $D^{*-} \to \overline{D}^0\pi^-$ decay. It is used for a measurement of the B^0 lifetime. The value obtained,

$$\tau_{B^0} = 1.529 \pm 0.012\ (\text{stat}) \pm 0.029\ (\text{syst})\ \text{ps},$$

is consistent with a recent *BABAR* measurement [4] and with the world average [5]. It is currently the most precise single measurement of this quantity.

We are grateful for the excellent luminosity and machine conditions provided by our PEP-II colleagues. The collaborating institutions wish to thank SLAC for its support and kind hospitality. This work is supported by DOE and NSF (USA), NSERC (Canada), IHEP (China), CEA and CNRS-IN2P3 (France), BMBF (Germany), INFN (Italy), NFR (Norway), MIST (Russia), and PPARC (United Kingdom). Individuals have received support from the Swiss NSF, A. P. Sloan Foundation, Research Corporation, and Alexander von Humboldt Foundation.

* Also with Università di Perugia, Perugia, Italy
† Also with Università della Basilicata, Potenza, Italy

[1] ARGUS Collaboration, H. Albrecht *et al.*, Phys. Lett. B **324**, 249 (1994); CLEO Collaboration, J. Bartelt *et al.*, Phys. Rev. Lett. **71**, 1680 (1993); DELPHI Collaboration, P. Abreu *et al.*, Z. Phys. C**73**, 299 (1997); DELPHI Collaboration, P. Abreu *et al.*, Z. Phys. C**76**, 579 (1997); DELPHI Collaboration, P. Abreu *et al.*, Phys. Lett. B**510**, 55 (2001); OPAL Collaboration, G. Abbiendi *et al.*, Phys. Lett. B**493**, 266 (2000); OPAL Collaboration, G. Abbiendi *et al.*, Phys. Lett. B**482**, 15 (2000).
[2] P.F. Harrison and H.R. Quinn, editors, "The *BABAR* Physics Book", SLAC-R-504.
[3] The *BABAR* Collaboration, B. Aubert *et al.*, SLAC-PUB-8569, hep-ex/0105044, accepted by Nucl. Instrum. Methods.
[4] The *BABAR* Collaboration, B. Aubert *et al.*, Phys. Rev. Lett. **87**, 201803 (2001).
[5] Particle Data Group, D.E. Groom *et al.*, Eur. Phys. Jour. C**15**, 1 (2000).

TABLE II: Contributions to the systematic error.

Source	$\sigma_{\tau_{B^0}}/\tau_{B^0}(\%)$
Continuum fraction & parametrization	0.36
$B\overline{B}$ fraction & parametrization	0.68
B^+ fraction & parametrization	0.64
Resolution model	1.14
Event selection bias	0.30
$\overline{D}^0$ bias ($\mathcal{R}_{\overline{D}^0}$)	0.95
Bias due to charm from the other B	0.21
z scale	0.40
Total	1.89